Planta _####################_
https://doi.org/10.1007/s00425-021-03633-0

ORIGINAL ARTICLE

Proteome impact on maize silks under the priming state induced by *Trichoderma* root colonization

Romina B. Agostini[1] · Sebastián P. Rius[1] · Walter A. Vargas[1,2] · Valeria A. Campos-Bermudez[1]

Received: 13 January 2021 / Accepted: 24 April 2021

Abstract

Main conclusion ***Trichoderma*** **activates plant proteins to counteract** ***Fusarium*** **infection. Comparison between proteomic and transcriptomic data suggests differential response regulation. Proteins from the phenylpropanoid pathway are activated to quickly respond to pathogen attack.**

Trichoderma species can stimulate local and distant immune responses in colonized plant tissues to prevent future pathogenic attacks. Priming of plant defenses is characterized by changes in transcriptional, metabolic, and epigenetic states after stimulus perception. We have previously investigated transcriptional reprogramming in silk tissues from maize plants inoculated with *Trichoderma atroviride* and challenged with *Fusarium verticillioides* (Agostini et al., Mol Plant-Microbe In 32:95–106, 2019). To better understand the molecular changes induced by *T. atroviride* in maize, a proteomic approach was conducted in this instance. Several proteins belonging to different metabolic categories were detected as priming-involved proteins. However, we detected a very low correlation with those priming-modulated transcripts suggesting the importance of regulatory events a posteriori of the transcriptional process to accomplish the final goal of blocking pathogen entry. Specifically, we focused on the phenylpropanoid pathway, since we detected several proteins that are upregulated in the priming state and might explain cell wall reinforcement as well as the increase in flavonoid and lignin content in maize silks after activation of induced systemic resistance.

Keywords Defense · *Fusarium* · Induced systemic response · Phenylpropanoids · Priming · Proteomic · *Trichoderma*

Abbreviations

DE	Differentially expressed
ISR	Induced systemic resistance
JA	Jasmonic acid
PAL	Phenylalanine ammonia-lyase
PR	Pathogenesis-related protein
SA	Salicylic acid
TmFm, TpFm, TmFp, TpFp	T = *Trichoderma,* F = *Fusarium*, m = minus, p = plus

Introduction

Trichoderma species are beneficial opportunistic fungi which can interact with roots of various plant species leading to induced systemic resistance (ISR) as a response to a wide spectrum of pathogens and adverse environmental conditions (Shoresh et al. 2010). Plant roots colonized by *Trichoderma* species can respond faster and/or thoroughly to pathogen attack following a mechanism known as priming, similar to the mechanism triggered by non-pathogenic rhizobacteria (Shoresh et al. 2010; Agostini et al. 2019).

Beginning with plant root attachment and followed by appressoria-like structure formation, the fungus gains access to internal plant tissues to set a beneficial plant–*Trichoderma* association (Yedidia et al. 2000). Plant symbionts have

Communicated by Dorothea Bartels.

✉ Valeria A. Campos-Bermudez
campos@cefobi-conicet.gov.ar

[1] Centro de Estudios Fotosintéticos y Bioquímicos (CEFOBI), Consejo Nacional de Investigaciones Científicas y Tecnológicas (CONICET), Universidad Nacional de Rosario, Suipacha 531, S2002LRK Rosario, Santa Fe, Argentina

[2] YPF-Tecnología, Av. del Petróleo Arg. S/N, 1923 Berisso, Argentina

developed specific strategies to promote colonization by evading the primary line of plant defense. Thus, different effector molecules are secreted into the apoplast or translocated into the plant cell cytoplasm where they interact with their molecular targets blocking downstream signals, thereby suppressing plant defense (Nogueira-Lopez et al. 2018). Finally, this symbiotic interaction leads to improved plant development and a quicker stress response.

The intrinsic mechanisms by which these beneficial microbes enhance both plant growth and systemic defenses remain a mystery. Focused on the ISR promoted by *Trichoderma*, transcriptional and proteomic studies have revealed a plethora of plant genes and proteins belonging to different metabolic pathways changing during this state. Despite these results are linked to specific interactions between different species of *Trichoderma* and plants, the most representative changes have been associated with phytohormone-regulated pathways, signal transduction and defense response mechanisms (Brotman et al. 2012; Mathys et al. 2012; Agostini et al. 2019).

Regarding hormone involvement in ISR induction, jasmonic acid (JA) and ethylene signaling in a salicylic acid (SA)-independent manner have been postulated in several systems. However, SA has also been implicated in ISR signaling for certain species (Salas-Marina et al. 2011; Pieterse et al. 2014). Additionally, oxylipins, methyl salicylate (MeSA) and redox-active small molecules including ROS and reactive nitrogen species were reported as relevant signals regulating ISR in plant resistance development (Park et al. 2007; Nawrocka et al. 2019; Wang et al. 2020).

The phenylpropanoid pathway is involved in secondary metabolism, present as a plant defense strategy and it is also activated in maize plants under the priming state (Mathys et al. 2012). This pathway is involved in the biosynthesis of many plant defense compounds, including flavonoids, lignin, condensed tannins, hydroxycinnamic acid and coumarins. In addition, phenylalanine ammonia-lyase (PAL) activity influences SA accumulation in several plant species such as arabidopsis, tobacco, pepper and soybean, thus regulating several responses triggered by this phytohormone (Ding and Ding 2020).

It is also generally assumed that *Trichoderma* spp. may trigger the extensive transcriptional reprogramming of plant genes involved in the production of phenolic compounds. These compounds despite displaying antioxidant and antimicrobial properties, enhance plant structural barriers preventing the spread of infection (Mandal et al. 2010). In this context, Nawrocka et al. (2018) also showed how *T. atroviride* induced callose and lignin deposition promoting mechanical plant strengthening. These compounds protected cells and dermal tissues in cucumber roots, shoots and leaves against *Rhizoctonia solani* making them more flexible and resilient.

To better understand the molecular basis of ISR our research is focused in the analysis of genomic and biochemical changes associated with the interaction of the tripartite system: *Zea mays—T. atroviride—F. verticillioides.*

F. verticillioides behaves as a symptomless intercellular endophyte and depending on environmental conditions, it can also become a hemibiotrophic pathogen in maize, although it has not conclusively been assigned any specific lifestyle (Christensen et al. 2014). Biotic and abiotic factors may alter the host-balanced relationship and produce a switch to the fungal pathogenic phases, finally causing plant spoilage accompanied by mycotoxin accumulation (Bacon et al. 2008). Contaminated seeds or rootlets infected by a soil-borne inoculum may transmit the pathogen to the newborn plants and kernels, while exogenous infections can occur by spore deposition on the maturing silks or through injuries caused by insects. Furthermore, *F. verticillioides* can produce fumonisins even during the symptomless state, and apparently healthy plants and kernels can be contaminated by these mycotoxins (Munkvold 2003). Some *Trichoderma* species have demonstrated their biocontrol capacity against *Fusarium* spp., which is more than relevant in these cases of endophytic pathogens (Ferrigo et al. 2014; Li et al. 2016; Saravanakumar et al. 2017).

We have exhaustively analyzed transcriptional reprogramming in maize silks together with the main hormonal pathways involved in ISR triggered by *T. atroviride* against *F. verticillioides* attack (Agostini et al. 2019). From that work we clarified that, in the priming condition, enhancement of pathogen perception is needed for a faster response to the imminent attack activating several host gene receptor-like brassinosteroid co-receptor BAK1 and numerous DUF26 family receptors. In addition, induction of transcripts related to antimicrobial metabolite synthesis (such as ROS, flavonoids and other secondary metabolites) and to defense-related genes (chitinase, thaumatin, glucanase, etc.) were associated with the ISR by *Trichoderma* to ward off *Fusarium* development. Furthermore, the importance of cell wall metabolism in the surveillance state of silks during ISR to delay further pathogenic invasion in maize cells was highlighted.

The most outstanding finding was an apparent combination of effects mediated by SA and JA signaling pathways along with no evidence of the activation of specific ET-related pathways in infected silks under ISR (Agostini et al. 2019). In that work, SA is accumulated in silks of *T. atroviride*-inoculated plants or after *F. verticillioides* infection. However, in primed plants after pathogen infection, a significant decrease in SA levels was observed. It was concordant with the observed downregulation of its biosynthetic pathway, and the transcriptional induction of salicylate/benzoate carboxyl methyltransferase responsible

Journal : Large 425 | Article No : 3633 | Pages : 17 | MS Code : 3633 | Dispatch : 28-4-2021

for the conversion of free SA into methyl salicylate (MeSA; Agostini et al. 2019).

Based on these previous results, we pursued a comparative analysis of the metabolic reprogramming at the proteomic level, together with the study of cell wall modifications (primary barrier), and concentration of the most relevant secondary metabolites in samples under the same treatments. These results will contribute to further understanding of metabolic changes in systemic tissues prompted by *Trichoderma* against pathogen attack.

Materials and methods

Fungal strains, plant material and experimental design

T. atroviride IMI206040 and *F. verticillioides* P364 isolates were grown as described (Agostini et al. 2019). *F. verticilloides* P364 was provided by Dr. Daniel Presello from EAA-INTA Pergamino, Argentina. *T. atroviride* was kindly provided by Prof. Charles M. Kenerley at Texas A&M University (USA). Plant material was obtained from *Zea mays* silks inbred line cv. B73 maintained in our lab. The experimental design consisted of seed inoculation with *Trichoderma* and silk infection with *Fusarium*. Experimental details were previously published (Agostini et al. 2019) and detailed in Fig. 1. Conditions under study were: (1) TmFm: silk samples without any fungal treatment (control condition); (2) TpFm: silk samples from seeds inoculated with *T. atroviride*; (3) TmFp: silk samples from *F. verticillioides*-infected plants; (4) TpFp: silk samples from *F. verticilliodes*-infected and *T. atroviride*-inoculated plants.

Sample preparation for microscopy

Samples were taken from silks and fixed in 50% (v/v) ethanol at 4 °C, 10% formaldehyde and 5% (v/v) acetic acid for 2 days. Samples were then dehydrated with ethanol solutions of increasing concentration and embedded in paraffin. Cross-sections (8 µm thick), were produced using a rotary microtome (Leica, Wetzlar, Germany) and placed onto gelatine-coated slides for microscopy. Sections were dewaxed and rehydrated with xylene followed by ethanol solutions of decreasing concentration and used for the staining procedures as follows.

Confocal microscopy

Samples were stained with 17.5 mg/ml calcofluor white (Sigma) during 5 min for cellulose detection. Sections were washed with 1× phosphate-buffered saline (PBS) pH 7.4 and mounted with anti-fade solution (0.1% (w/v) *p*-phenylenediamine and 50% (v/v) glycerol in 1× PBS). The stained material was observed under a microscope Nikon Eclipse TE-2000-E2 with the confocal system Nikon C1Plus SiR using the following settings: excitation = 405 nm; emission = 450/35 nm (blue). Images were acquired with the Nikon EZ-C1 software. Epidermal cells from five silks were analyzed. Cell wall width was measured using the "Image J" program in sections at 90º with respect to the cell wall perimeter. Plots were constructed with BoxPlotR, a web tool for box plot generation.

Histochemical localization and quantification of lignin

Dewaxed and rehydrated samples were placed in 2% phloroglucinol in 95% ethanol for 2 h. Tissues were subsequently placed in a drop of 35% HCl on a slide and observed under high power (100×) microscope magnification. Images were analyzed using the "Image J" program. This program allowed us to determine the contribution of each channel to the image by studying the channels called RGB (red, green and blue). By analyzing the RGB channels of an image selection, we were able to quantify (count) the number of pixels with each color value (between 0 and 255) detectable in each channel (RGB). Thus, a histogram (number of pixels for each value) was obtained. The red intensity was determined as the average value of the histogram corresponding to this color. Boxplots were constructed with BoxPlotR, a web tool for boxplot generation.

Quantification of phenolics

Different amounts of pulverised tissue (0.05–0.1 g of dried weight of silks) were incubated ON at 4 °C in 1 ml extraction buffer (0.5 M HCl in 80% v/v methanol) for the extraction of phenolic compounds. Then, extracts were centrifuged for 20 min at 12,000×*g* and 4 °C. The supernatant volume was measured and the supernatant transferred to another tube. AQ2

Extracts (15 µl and 25 µl) obtained from 0.05 g of tissue were diluted to a final volume of 150 µl with H_2O for the determination of phenolic compounds. Folin reagent (Merck, 150 µl) was added and incubated at room temperature for 3 min. 1 M Na_2CO_3 (300 µl) was added, mixed by gentle inversion and left to stand for 1 h at 20 °C. Absorbance was measured at 725 nm in a Jasco V-630 spectrophotometer. Gallic acid was used as standard and a calibration curve was constructed. Boxplots were obtained using the BoxPlotR web tool.

Statistical analysis

Sigma Stat Package (Systat Software Inc., San Jose, CA, USA) was used for data analysis. Tukey's test ($\alpha = 0.05$) was

Journal : Large 425 | Article No : 3633 | Pages : 17 | MS Code : 3633 | Dispatch : 28-4-2021

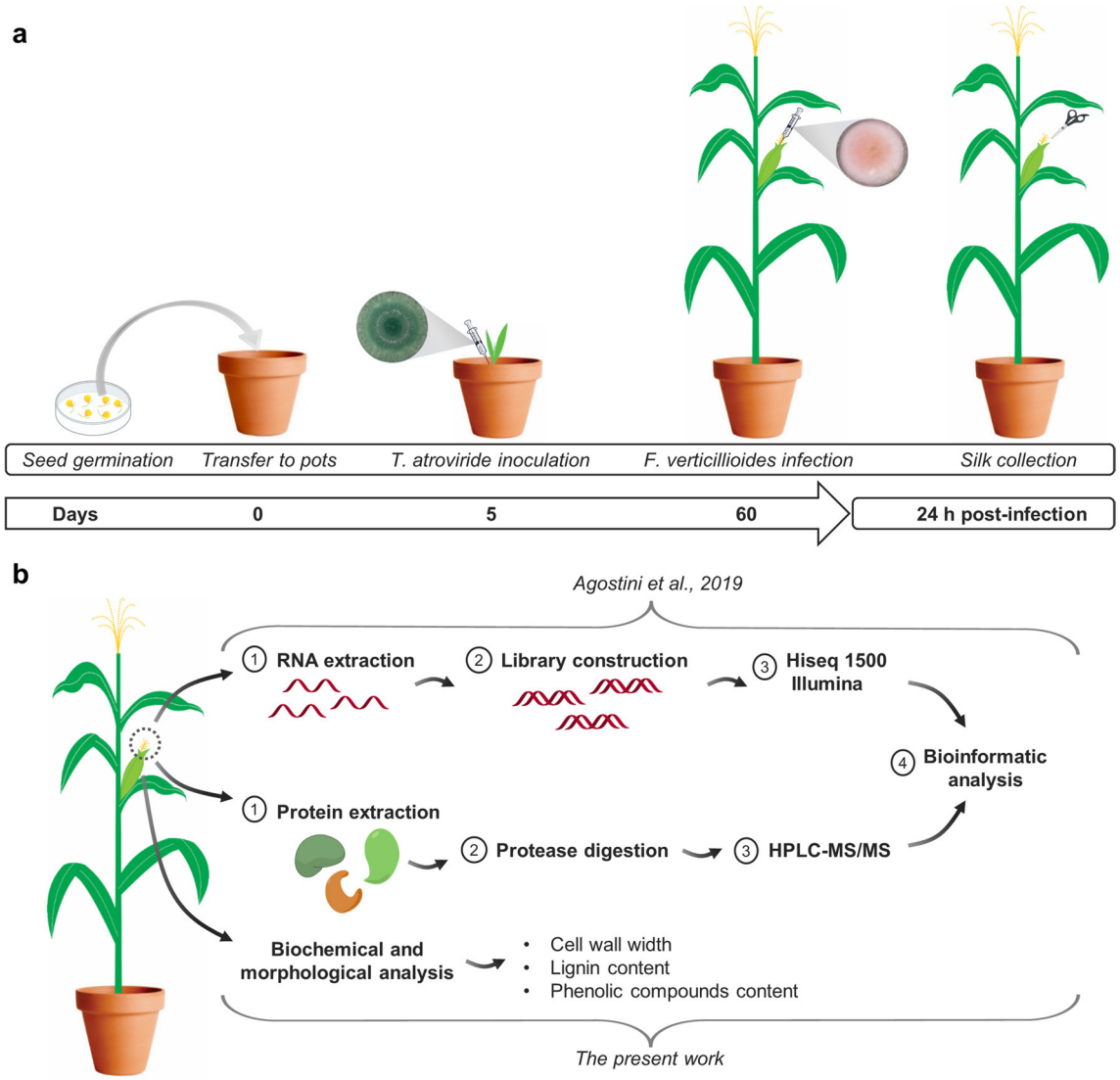

Fig. 1 **a** Experimental design for *T. atroviride*-inoculation and *F. verticillioides* infection. Sampling was performed 24 h post-infection. **b** Collected silks were subjected to three parallel processes: transcriptome analysis by RNA-seq (Agostini et al. 2019), proteome analysis by HPLC–MS/MS and biochemical and morphological analysis (present work)

used for comparison of cell wall width measurements, red intensity determination (indirect quantification of lignin) and phenolic levels among the four conditions under study.

Protein extraction

Soluble protein extracts from maize silks, were obtained from 100 mg of tissue pulverized with liquid N_2 and homogenized in one volume of extraction buffer containing 50 mM Tris–HCl, pH 8.0, 5 mM EDTA, 0.1% (v/v) Triton X-100 and 2 mM PMSF. The homogenate was incubated for 30 min on ice and then centrifuged at 14,000×*g* for 20 min at 4 °C. Supernatants were transferred to empty tubes and saved. The supernatant protein concentration was determined spectrophotometrically by the Bradford method using the Protein Assay (BioRad) dye reagent using bovine serum albumin as standard.

Extracts (10 µg of protein) were separated on SDS–polyacrylamide gel electrophoresis (SDS-PAGE) to check for protein stability.

Sample preparation for proteomic analysis

Protein crude extracts (100 µg) were precipitated with 1:5 vol of 100% (w/v) trichloroacetic acid (TCA) for 2 h at 20 °C, and then centrifuged at maximum speed for 20 min. Protein pellets were dissolved in 50 µl of 8 M urea. Denatured proteins were then reduced with 10 mM dithiothreitol

Journal : Large 425 | Article No : 3633 | Pages : 17 | MS Code : 3633 | Dispatch : 28-4-2021

(DTT) (45 min at 56 °C) and treated with 20 mM iodoacetamide (60 min at room temperature in the dark) to prevent disulfide bonds reformation and finally precipitated with TCA (1/5 100% P/V).

HPLC–MS/MS and protein identification and quantification

Pellets were analyzed at the Center of Biological and Chemical Studies by Mass Spectroscopy (CEQUIBIEM, Buenos Aires, Argentina), for further protein identification and quantification. A solution of 50 mM NH_4HCO_3, pH 8.0, was used to resuspend proteins for overnight digestion with sequencing-grade modified trypsin (Promega). Zip-Tip C18 (Merck Millipore) columns were used for desalting. Peptides were separated in a nano-HPLC (EASY-nLC 1000, ThermoScientific) coupled to a mass spectrometer with Orbitrap technology (Q-Exactive with High Collision Dissociation cell and Orbitrap analyser, ThermoScientific). Peptides were ionized by electrospray (ThermoScientific, model EASY-SPRAY). Proteome Discoverer 2.1 software (ThermoScientific) and the maize reference proteome set from Uniprot (*Zea mays*, strain: cv. B73—UP000007305—Uniprot) were used for protein identification and relative quantitation. UniprotKB accession number (http://www.uniprot.org/uniprot/), score, coverage, peptides used for identification, description, area in each biological repetition; as well as other parameters for each protein obtained from the Proteome Discoverer software, are listed in Supplementary Table S1. The mass spectrometry proteomics data have been deposited to the ProteomeXchange Consortium via the PRIDE partner repository with the dataset identifier PXD024698 (Perez-Riverol et al. 2019).

Statistical analysis of proteomics data

Perseus 1.5.8.5 software was used for statistical analysis of proteomics data. Data were normalized and subjected to manually missing-value imputation. When at least two of the three replicates were missing/zero, they were replaced by the minimum value detected by the mass spectrometer (considered as the detection limit). Instead, when the peptide was detected in two of the three replicates the missing/zero values were left blank. Label-free quantification (LFQ) protein intensities were $\log_2$ transformed. Two-sample tests were conducted to compare proteomes for each condition (TpFm, TmFp, TpFp) vs. the control (TmFm) by applying the standard *t* test statistic with a permutation-based false discovery rate of 0.05. Proteins with a *P* value ≤ 0.05 and a $\log_2$ (fold change) $>|1|$ were considered as significantly differentially expressed (DE). Volcano plots showing $-\log$ (*P* values) were used to assess differences in TpFm vs. TmFm, TmFp vs. TmFm and TpFp vs. TmFm. Differential proteins are listed in Supplementary Table S2. In addition, UniprotKB accession, Gene Name, $\log_2$ (FC) and $-\log$ (*P* value) for each protein in each condition, and description are indicated in this table.

Analysis of differentially expressed proteins

Differentially expressed proteins were visualized and functionally analyzed using the MapMan 3.6.0 Software. Prior to this analysis, it was essential to assign the geneID to each protein, making use of the Biomart platform (accessible from Phytozome v12.1.5, https://phytozome.jgi.doe.gov/pz/portal.html).

Selection of priming proteins

Selection of priming proteins was performed in the same way as for priming gene selection (Agostini et al. 2019). This selection included all the proteins exclusively up- or downregulated in the TpFp/TmFm comparison as well as those with a significant DE both in TpFp/TmFm and TmFp/TmFm comparisons. These priming proteins are listed in Supplementary Table S3. UniprotKB accession, GeneID, $\log_2$ (FC) and $-\log$ (*P* value) for each protein in each condition, description and Gene-Ontology (GO) are indicated in this table. Analysis of genetic ontology was carried out using the AgriGo platform (http://bioinfo.cau.edu.cn/agriGO/).

Analysis of the phenylpropanoid pathway

CornCyc 9.0 (https://corncyc-b73-v4.maizegdb.org/) and KEGG PATHWAY Database (https://www.genome.jp/kegg/pathway.html) were used to analyze the phenylpropanoid pathway and identify priming proteins involved in it.

Results

Physiological changes in silk samples after *Trichoderma* inoculation and/or *Fusarium* infection

We focused on the study of ISR triggered by *T. atroviride* in maize silks. For this purpose, we proposed an experimental design based on the tripartite system *Zea mays—T. atroviride—F. verticillioides* (Fig. 1a). Silk samples from plants without any treatment correspond to the control condition and were named TmFm, while TpFp corresponds to silk samples subjected to both treatments. TpFm refers to silk samples from maize plants previously inoculated with *T. atroviride* and TmFp to silk samples from *F. verticillioides*-infected plants. In this way, silk samples under different treatments previously analyzed by a genetic approach

Journal : Large 425 | Article No : 3633 | Pages : 17 | MS Code : 3633 | Dispatch : 28-4-2021

(Agostini et al. 2019) were now also studied through proteomic, biochemical and morphological approaches (Fig. 1b).

Microscopic confocal analysis of silk cell wall

Considering the relevance of cell wall structure as first defense barrier to prevent the entry and spread of pathogens and as a probable mechanism of ISR by *Trichoderma*, confocal microscopy was used to obtain information regarding cell wall features in epidermal cells. Thus, silks from different treatments were stained with Calcofluor dye (Fig. 2a) and wall width of epidermal cells was determined as described in "Materials and methods". Results are shown in Fig. 2.

We observed a statistically significant increase ($P < 0.05$) in cell wall width for plants infected with *Fusarium* (TmFp) compared to the control (TmFm) (Fig. 2b). In other words, the plant is sensing the presence of the pathogen and responding through modifications on the primary entry barrier. On the other hand, inoculation with *Trichoderma* (TpFm and TpFp conditions) also induced a statistically significant increase ($P < 0.05$) in cell wall width when compared to the control (TmFm). Differences are even more noticeable when compared to the condition in which only infection with the pathogen (TmFp) was performed. This evidence would indicate once again the involvement of *T. atroviride* on cell wall reinforcement in the long-lasting ISR developed in maize plants. It should be noted that *Trichoderma* inoculation is carried out in roots and reinforcement is evidenced 2 months later on a distant tissue.

Histochemical localization and quantification of lignin content in silks

Based on the previous results concerning cell wall width (Fig. 2), histochemical localization of lignin in maize silks was performed using phloroglucinol. Optical microscope observations detected the presence of lignin by the appearance of a reddish color in the cell wall. Lignin content was quantified through red intensity measurement using the program "Image J" (Fig. 3).

Surprisingly, after 24 h of *Fusarium* infection (TmFp condition), no statistically significant change in red intensity with respect to the control (TmFm) was detected. That is, changes in lignin content in the cell wall of silks infected with the pathogen were not detected by this method. However, the results obtained revealed a statistically significant increase ($P < 0.05$) in the average red intensity in the TpFp condition with respect to the control condition (TmFm). This allows us to infer that lignin content in silks increased as result of *Trichoderma*

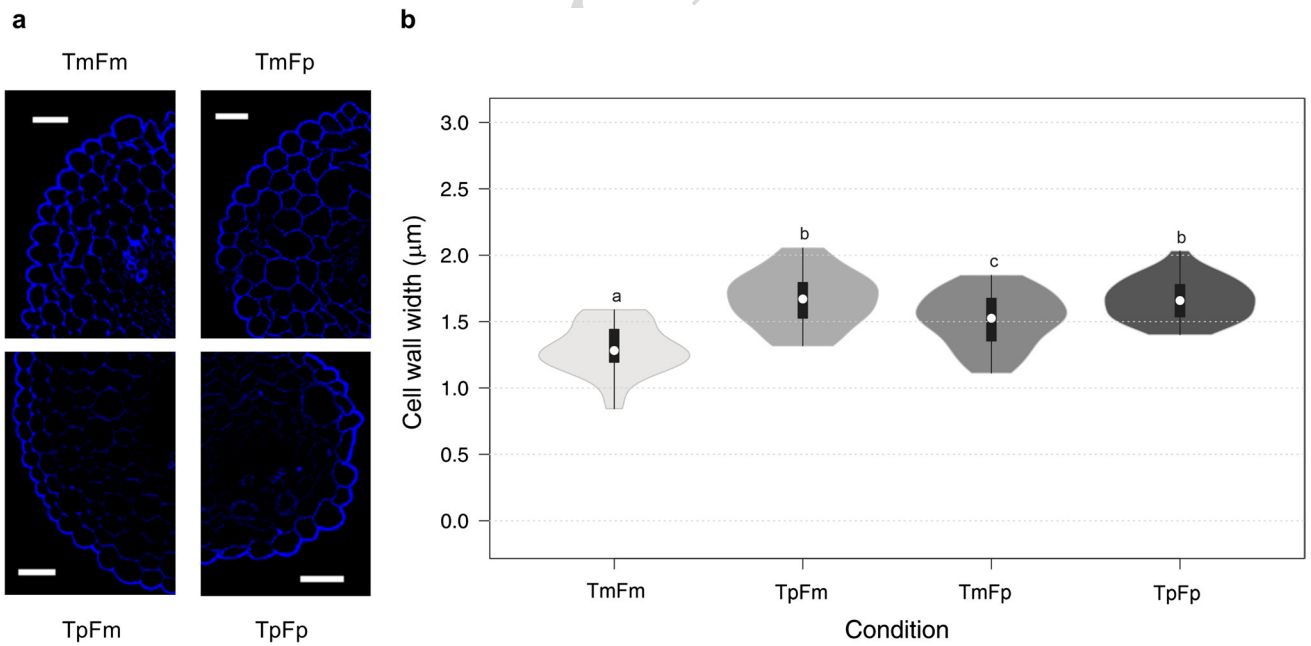

Fig. 2 Microscopic confocal analysis of silk epidermal cells after Calcofluor staining. **a** Control condition (TmFm), *Trichoderma* root-inoculated plants (TpFm), *Fusarium*-infected plants (TmFp) and *Trichoderma*-inoculated and *Fusarium*-infected plants (TpFp). Scale bars: 30 µm. **b** Violin plots of cell wall thickness in epidermal cells from transversal sections of silks in the four conditions under study. Cell wall width was quantified using confocal laser scanning microscopy images of Calcofluor-stained sections collected in the blue channel. Cell wall width was measured using the program "Image J" (http://imagej.nih.gov/ij) in sections at 90º with respect to cell wall perimeter. Plots were constructed with the BoxPlotR web tool. Violins with different letters vary considerably at a significance level of 5% according to Tukey's test

Journal : Large 425 | Article No : 3633 | Pages : 17 | MS Code : 3633 | Dispatch : 28-4-2021

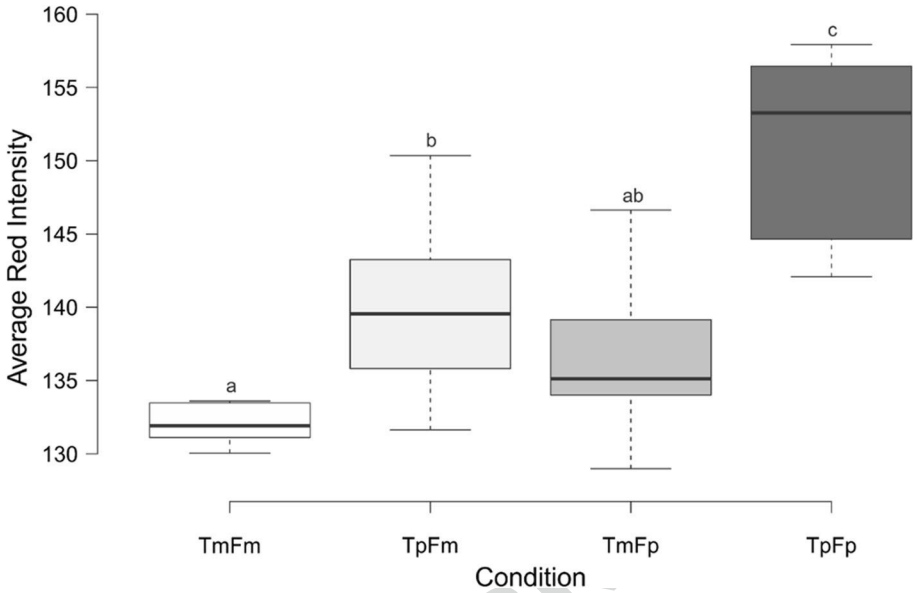

Fig. 3 Quantification of lignin content in control (TmFm), *Trichoderma*-inoculated (TpFm), *Fusarium*-infected (TmFp) and *inoculated + infected* (TpFp) maize silks. Lignin deposited on the silk cell wall was visualized as a red stained material. The red color was quantified using the program "Image J" (http://imagej.nih.gov/ij). Boxplots were constructed using the BoxPlotR web tool. Boxplots with different letters vary markedly with a significance level of 5% according to Tukey's test

inoculation and *Fusarium* infection. Interestingly, the red intensity in the condition in which only *Trichoderma* inoculation was performed (TpFm) was higher than in the control condition (TmFm) but lower than in the TpFp condition. These results suggest that *Trichoderma* inoculation induces an increase in lignin accumulation in the priming state. Such increase is even greater after pathogen attack, thus contributing to the strengthening of the primary defense barrier.

Quantification of phenolic compounds in maize silks

Quantification of phenolic compounds was carried out to corroborate the incidence of these secondary metabolites in the ISR triggered by *Trichoderma*. Results are shown in Fig. 4. A statistically significant increase ($P < 0.05$) in phenolics concentration was evidenced under inoculation and/or infection conditions (TpFm, TmFp and TpFp) compared to the control (TmFm). However, no statistically significant difference was detected among them. Similar results were observed for flavonoid content determination (data not shown).

These results indicate that both inoculation with *Trichoderma* and pathogen infection, generate an increase in the concentration of these compounds. Such changes are produced to protect and confer resistance to the plant against pathogen attack. It is worth mentioning that root inoculation with *Trichoderma* also generates an increase in these plant compounds systemically. This is the result of the ISR activation which in turn prepares the plant for future pathogen attacks.

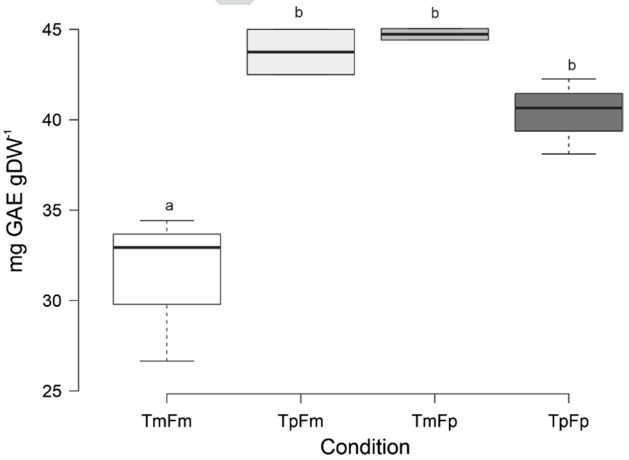

Fig. 4 Determination and quantification of phenolics in maize silks. This experiment was performed under the four conditions described: TmFm, TpFm, TmFp and TpFp. Phenolic compound concentration is represented as milligrams of gallic acid equivalents (GAE)/ dried weight (DW) of silks. Graphs were constructed using the BoxPlotR web tool. Boxplots with different letters vary markedly with a significance level of 5% according to Tukey's test

Silk differential proteomics from *Trichoderma*-inoculated and *Fusarium*-infected maize plants

To study the effects and the key regulatory pathways involved in the priming of the plant immune system, we performed a study of proteomics through mass spectrometry in silk samples under the four previously mentioned conditions (Fig. 1).

Journal : Large 425 | Article No : 3633 | Pages : 17 | MS Code : 3633 | Dispatch : 28-4-2021

After identification (Proteome Discoverer) and statistical analysis (Perseus), results obtained revealed a total of 622 differentially expressed proteins (DE) ($P < 0.05$ and $\log_2$ (FC) >|1|) in at least 1 of the observations compared to the control condition. As observed in the Volcano plots (Supplementary Fig. S1), 285 proteins modulated by *T. atroviride*-inoculation were identified from the comparison between the proteomic profile of samples from the TpFm treatment and the control condition TmFm (TpFm/TmFm) (Supplementary Fig. S1a). After comparing TmFp and TmFm, 346 proteins responding to *F. verticillioides* infection were distinguished (Supplementary Fig. S1b). In addition, 389 proteins modulated by *Trichoderma* inoculation and *Fusarium* infection were detected in the TpFp/TmFm analysis (Supplementary Fig. S1c).

Analyzing these data through Venn Diagrams (Fig. 5a), we observed that 93 DE proteins are common in the 3 comparisons (TpFm/TmFm, TmFp/TmFm and TpFp/TmFm), 50 proteins are common between TpFm/TmFm and TmFp/TmFm comparisons and 53 proteins are present in TpFm/TmFm and TpFp/TmFm. However, the greatest amount of DE proteins (109) was found when comparing TmFp/TmFm and TpFp/TmFm.

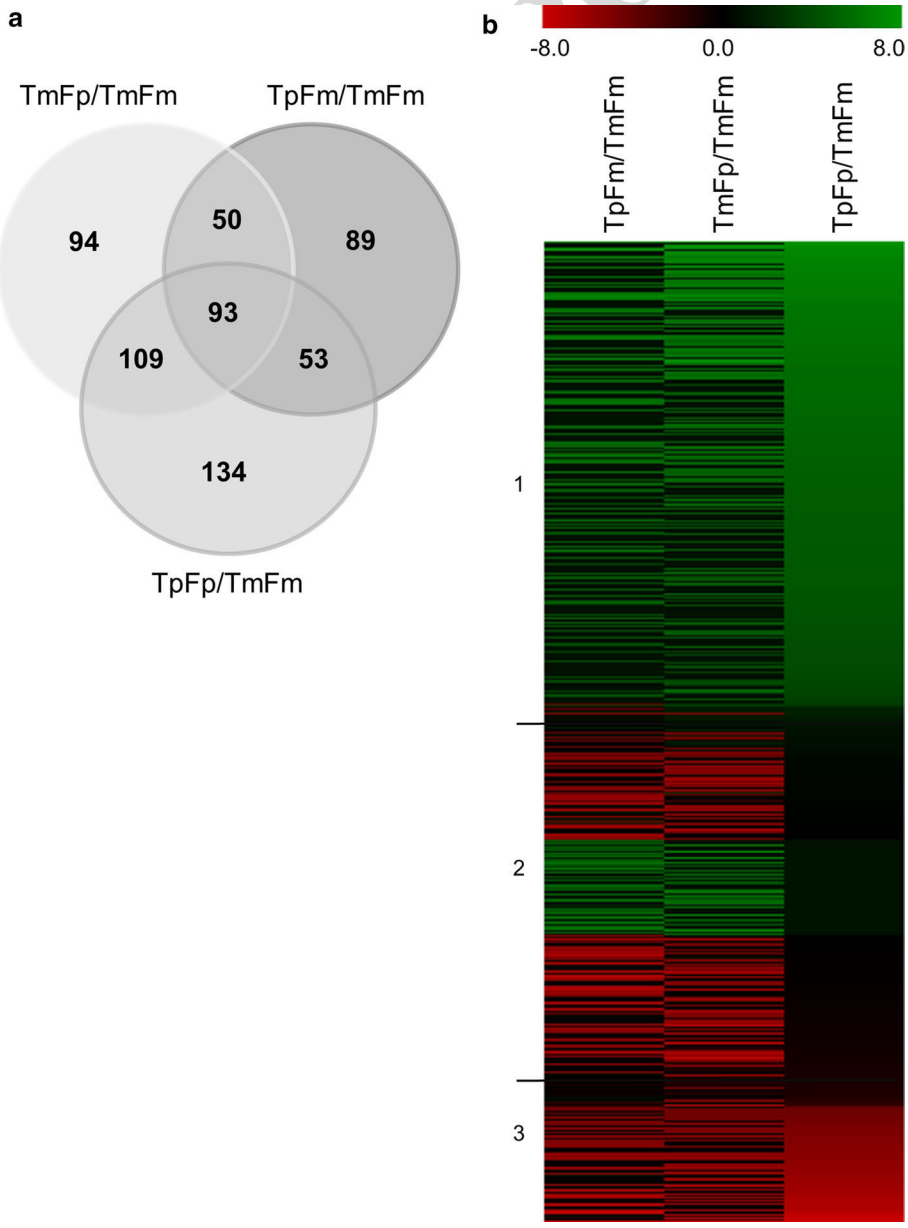

Fig. 5 **a** Venn diagram summarizing the distribution of the 622 differentially expressed (DE) proteins among the three comparisons under study: TpFm/TmFm, TmFp/TmFm and TpFp/TmFm. **b** Heatmap of DE proteins. Cluster 1: upregulated proteins ($\log_2$ (FC) > 1 and $P < 0.05$) in the *Trichoderma* inoculation and *Fusarium* infection condition compared to the control (TpFp/TmFm). Cluster 2: no DE proteins in the TpFp/TmFm comparison. Cluster 3: downregulated proteins ($\log_2$ (FC) < − 1 and $P < 0.05$) in the TpFp/TmFm comparison

Journal : Large 425 | Article No : 3633 | Pages : 17 | MS Code : 3633 | Dispatch : 28-4-2021

Early translation changes in maize silks after pathogen challenge in plants under the priming state elicited by *Trichoderma* pre-treatment

We made a selection of priming proteins, under the same criterion previously applied for priming genes (Agostini et al. 2019). These included all the proteins that appear exclusively in the TpFp/TmFm comparison, as well as those that show significant DE in both TpFp/TmFm and TmFp/TmFm situations. These are included in cluster 1 and 3 of the heatmap (Fig. 5b). Thus, we have identified 336 proteins involved in defense enhancement of maize plants against *F. verticillioides*, elicited by *Trichoderma*. Priming-related proteins are listed in Supplementary Table S3.

To analyze the functional identity of priming proteins, the MapMan 3.6.0 software was used and a graph constructed to represent the enrichment in each of the described categories (Fig. S2). As shown in Fig. S2, the response mediated by the ISR mainly involves activation at the translation level, being the most enriched functional classifications: *energetic metabolism*, *structure and metabolism of cell wall*, *amino acid and protein metabolism*, *response to stress*, *miscellaneous and unassigned* (with 5.2%, 5.0%, 17.9%, 7.4%, 7.4% and 9.8% of upregulated proteins, respectively). *Amino acid and protein metabolism* category was also the most enriched in downregulated proteins (6.4%).

A schematic description of changes observed in protein expression under the three treatments in their most relevant metabolic context is depicted in Fig. 6. Further enumeration of most relevant proteins in each category is commented.

Priming proteins involved in secondary metabolism

Proteins belonging to terpene, flavonoid, phenylpropanoid and phenolic biosynthetic pathways were analyzed (Fig. 6). These metabolisms are extremely appealing due to their involvement in antimicrobial and defense compound synthesis.

Terpenes. All proteins selected as involved in the priming state and classified within terpene metabolism were upregulated. Hydroxymethylglutaryl-CoA synthase (GRMZM2G106263) is the second enzyme in the mevalonate (MVA) pathway of isoprenoid biosynthesis and it plays an important role in phytosterol biosynthesis. In addition, deoxy xylulose reductoisomerase 1 (GRMZM2G056975) and hydroxymethylbutenyl diphosphate synthase 1 (GRMZM2G137409), both involved in

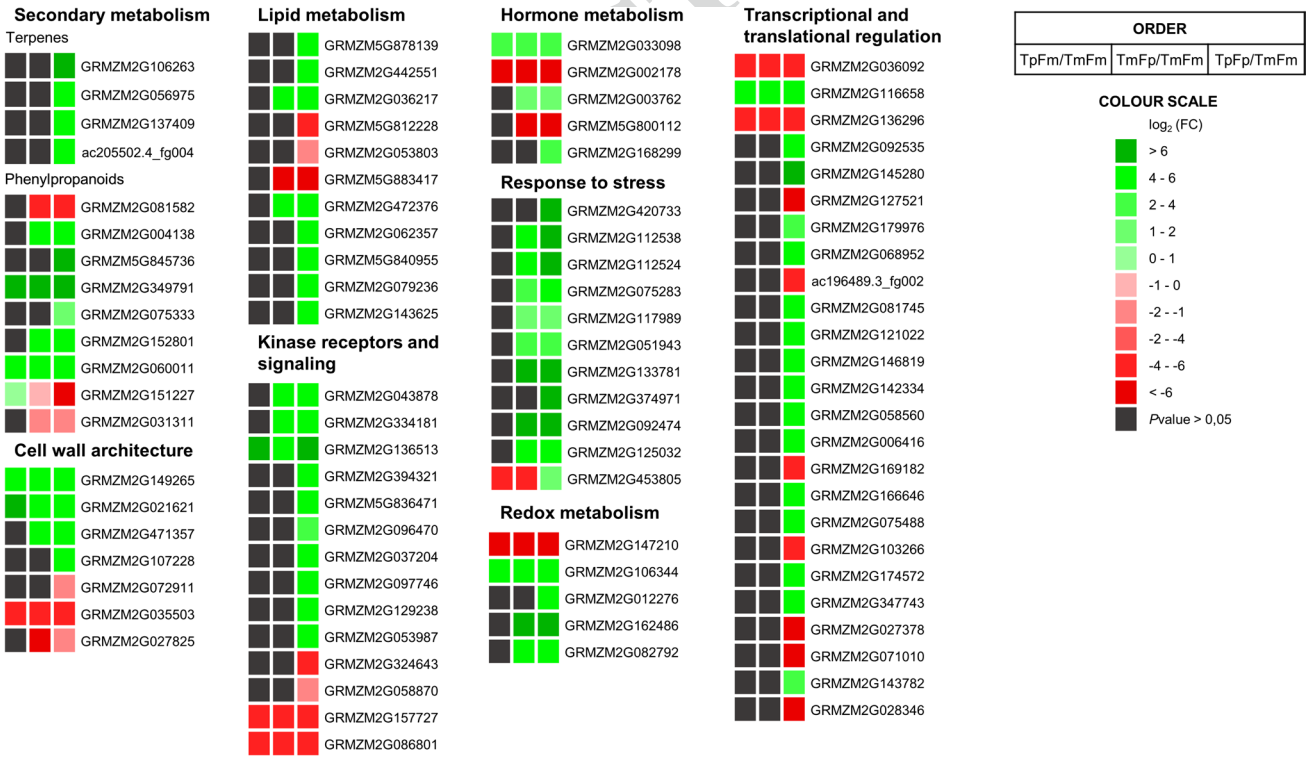

Fig. 6 Protein profile changes of selected priming-related proteins from maize silks under different treatments. Translational variations are represented in a red–green scale. Green and red boxes indicate up- and downregulated proteins, respectively. Black boxes indicate *P* value > 0.05. The first box corresponds to the TpFm/TmFm condition, while the second and third to TmFp/TmFm and TpFp/TmFm conditions, respectively

Journal : Large 425 | Article No : 3633 | Pages : 17 | MS Code : 3633 | Dispatch : 28-4-2021

the isoprenoid biosynthetic process, are part of an alternative mevalonate-independent 2-*C*-methyl-D-erythritol 4-phosphate (MEP) pathway for the formation of isopentenyl diphosphate (IPP). Furthermore, α-humulene synthase (ac205502.4_fg004), with terpene synthase activity, was also found in priming gene selection (Agostini et al. 2019), showing the same expression pattern.

Phenylpropanoids. Plant-derived phenylpropanoids are precursor molecules for biosynthesis of numerous structurally and functionally diverse plant polyphenols (simple phenolic acids and esters, glycosylated derivatives of primary phenylpropanoids, flavonoids, isoflavonoids, stilbenes, coumarins, curcuminoids, lignans, etc.), which play several essential roles in plant physiology. Regarding this metabolic pathway (Fig. 7), we have detected that phenylalanine ammonium lyase (PAL) (GRMZM2G081582) was downregulated. However, other proteins were upregulated, such as caffeoyl-CoA O-methyltransferase 1 (CCoAOMT, GRMZM2G004138, associated with lignin biosynthesis), β-glucosidase (GRMZM5G845736), O-methyltransferase ZRP4 (GRMZM2G349791) and 4-coumarate-CoA ligase 1 (GRMZM2G075333). β-glucosidase is an enzyme involved in coumarin biosynthesis, while O-methyltransferase ZRP4 is involved in the salvigenin (5-hydroxy-6,7,4′-trimethoxyflavone) synthetic pathway, and closely associated with production of both monolignols and ferulates (Riboulet et al. 2009). The 4-coumarate:CoA ligases (4CLs, EC 6.2.1.12) are a group of enzymes necessary to maintain a continuous metabolic flow for phenylpropanoid biosynthesis, including compounds such as lignin and flavonoids, which are essential for plant survival.

Concerning the flavonoid synthetic pathway (Fig. 7), we identified two upregulated proteins in priming conditions: flavonol synthase 1 (GRMZM2G152801) and chalcone isomerase (GRMZM2G060011). However, chalcone synthase WHP1 (GRMZM2G151227) was downregulated in the priming state. This behavior correlates with previous observations at the transcriptional level in the published RNA-seq experiment (Agostini et al. 2019). Finally, salmon silk-1 (SM1, GRMZM2G031311) was downregulated. This protein is involved in the last step of the maysin (C-glycosyl flavone) biosynthetic pathway.

This evidence indicates that there is significant reprogramming in secondary metabolism during the ISR response in maize silks. These secondary metabolites could be produced to more effectively counteract the attack by the pathogen *F. verticillioides* in previously elicited plants.

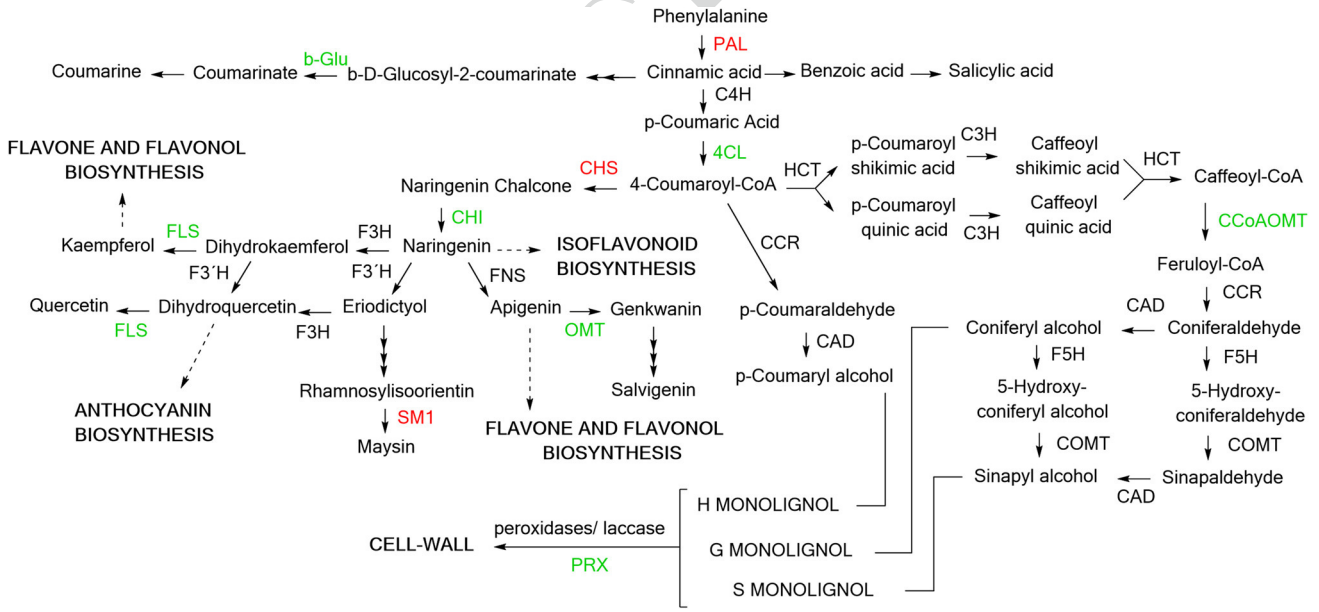

Fig. 7 The phenylpropanoid pathway in maize. *4CL* 4-coumarate:CoA ligase (GRMZM2G075333), *b-Glu* β-glucosidase (GRMZM5G845736), *C3H* *p*-coumarate 3-hydroxylase, *CAD* cinnamyl-alcohol dehydrogenase, *CCoAOMT* caffeoyl-CoA *O*-methyltransferase (GRMZM2G004138), *CCR* cinnamoyl-CoA reductase, *C4H* cinnamate 4-hydroxylase, *CHI* chalcone isomerase (GRMZM2G060011), *CHS* chalcone synthase (GRMZM2G151227), *COMT* caffeic acid *O*-methyltransferase, *F3'H* flavonoid 3′-hydroxylase, *F3H* flavanone 3-hydroxylase, *F5H* ferulate 5-hydroxylase, *FLS* flavonol synthase (GRMZM2G152801), *FNS* flavone synthase, *G monolignol* lignin guaiacyl unit, *HCT* hydroxycinnamoyl-CoA transferase, *H monolignol* *p*-hydroxyphenyl lignin unit, *OMT* *O*-methyltransferase (GRMZM2G349791), *PAL* phenylalanine ammonia-lyase (GRMZM2G081582), *PRX* peroxidase (GRMZM2G107228 and GRMZM2G471357), *S monolignol* syringyl lignin unit, *SM1* salmon silk-1 (GRMZM2G031311). Priming proteins are colored: red (downregulated) and green (upregulated)

Journal : Large 425 | Article No : 3633 | Pages : 17 | MS Code : 3633 | Dispatch : 28-4-2021

Priming proteins involved in cell wall architecture

This primary barrier is crucial to prevent the entry and spread of pathogens. Therefore, reorganizations and modifications are accomplished to reinforce the cell wall during attack by invading pathogens (Fig. 6). Moreover, besides the above-mentioned proteins involved in the phenylpropanoid pathway (Fig. 7), several other proteins appear as involved in cell wall rearrangement. We have found several upregulated proteins in priming conditions, such as mannose-1-phosphate guanylyl transferase 1 (GRMZM2G149265), β-expansin 2 (GRMZM2G021621), and some peroxidases (GRMZM2G471357 and GRMZM2G107228). Mannose-1-phosphate guanylyl transferase 1 plays an essential role in plant growth and development as well as in cell wall architecture, since it provides GDP-mannose, used for cell wall carbohydrate biosynthesis. β-Expansin proteins are known to display cell wall loosening activity along with an involvement in cell expansion and other developmental events during which cell wall modification occurs. Finally, both peroxidases, in addition to removing H_2O_2, are involved in the last step of the lignin biosynthetic pathway (Fig. 7). We have also found three downregulated proteins in this condition, such as bifunctional dTDP-4-dehydrorhamnose 3,5-epimerase/dTDP-4-dehydrorhamnose reductase (GRMZM2G072911) involved in UDP-β-L-rhamnose biosynthesis, a putative β-D-xylosidase 7 (GRMZM2G035503) involved in cell wall degradation and an uncharacterized protein (GRMZM2G027825) that contains a FAS 1 (fasciclin-like) domain, and is highly similar to fasciclin-like arabinogalactan protein 16.

Priming proteins involved in lipid metabolism

In response to pathogen attack, membrane fluidity modifications are triggered and lipid compounds acting in signal transduction processes released. Regarding this metabolism, we detected the following proteins as upregulated by priming: acyl-activating enzyme 17 peroxisomal (GRMZM2G472376), putative acyl-activating enzyme 18 peroxisomal (GRMZM2G062357), long-chain acyl-CoA synthetase 8 (GRMZM5G840955), long-chain acyl-CoA synthetase family member 3 (GRMZM2G079236); an acyl desaturase (GRMZM2G143625), 1-acyl–sn–glycerol-3-phosphate acyltransferase (PLS, GRMZM5G878139), phospholipase D5 (PLD, GRMZM2G442551) and a fatty acyl-CoA reductase (FAR, GRMZM2G036217) (Fig. 6). FARs catalyze the formation of a long-chain primary fatty alcohol from a long-chain fatty acyl-CoA and NADPH. The resulting long-chain primary alcohols are significant components in cuticle waxes of plants. On the other hand, PLD is the enzyme responsible for hydrolyzing structural phospholipids giving rise to phosphatidic acid (PA), an important signal molecule in response to various types of stress, both biotic and abiotic (Testerink and Munnik 2005).

At the same time, three downregulated proteins involved in the synthesis and elongation of fatty acids, were observed. Long-chain-fatty-acid-CoA ligase (GRMZM5G812228), acyl-CoA-binding protein (ACBP, GRMZM2G053803) and stearoyl-acyl-carrier-protein desaturase 8 (SAD8, GRMZM5G883417). Cytosolic ACBP binds long-chain acyl-CoA esters, act as intracellular acyl-CoA transporter and maintains acyl-CoA pools. With regard to SAD, it is responsible for the first desaturation step leading to oleic acid, which can be further desaturated to linoleic and α-linolenic acids. Therefore, SAD activity is important in determining the overall content of unsaturated fatty acids (UFA). These fatty acids, besides representing the major source of energy in the form of triacylglycerols, also constitute complex lipids that are essential components of cellular membranes. Plant UFAs and their derivatives have been proposed as signaling molecules involved in the response to biotic and abiotic stresses (Kachroo and Kachroo 2009).

These results reveal a significant modification in lipid metabolism in response to ISR, probably to block entry through the membrane and intervening in signal transduction pathways to trigger defense responses quickly.

Kinase receptors and signaling

In terms of signal perception, we have found several specific kinase receptors with pathogen-sensing activity located on the cell wall, such as leucine-rich receptors (LRR), DUF26 and cysteine-rich receptors (CRK), as well as key components linked to signaling and signal transduction. We have also identified two upregulated DUF26 domain family proteins (GRMZM2G043878 and GRMZM2G334181). These two proteins, namely AFP1 and AFP2 (Anti-Fungal Protein 1 and 2), have been reported to recognize and react to various pathogenic fungi. Specifically, maize plants silenced for these two receptors were significantly more susceptible to infection by *Ustilago maydis* SG200 and *Colletotrichum graminicola* (Ma et al. 2018). Therefore, it is probable that *Trichoderma* increases the expression of these receptors with the aim of improving pathogen perception. Additionally, we have found the upregulated immune receptor disease resistance protein (GRMZM2G136513) also known as RPS5 (Resistance to *Pseudomonas syringae* 5). It is a typical nucleotide-binding domain leucine-rich repeat (NLR) protein. NLRs act as intracellular receptors to recognize pathogen effectors (Pottinger and Innes 2020).

On the other hand, a probable inactive receptor kinase (GRMZM2G394321), ABC transporter G family member 5 (GRMZM5G836471), Ypt/Rab-GAP domain of the gyp1p superfamily protein (GRMZM2G096470) and two Ras-related proteins RABD2c (GRMZM2G037204 and

Journal : Large 425 | Article No : 3633 | Pages : 17 | MS Code : 3633 | Dispatch : 28-4-2021

GRMZM2G097746) were upregulated in the priming state. ABC proteins are widely involved in immune system regulation, intermediate metabolite manipulation, tissue establishment, hormone transport and signaling, drug resistance, and abiotic stress accommodation, all of which have the potential to improve agricultural production (Borghi et al. 2019). The Ypt/Rab GTPases are key regulators of protein transport in all eukaryotic cells, particularly involved in vesicle trafficking and formation, motility, docking and membrane remodeling and fusion (Segev 2001).

In addition, the upregulated phosphoinositide phospholipase C (PLC, GRMZM2G129238) was detected in the priming condition. Although this enzyme belongs to lipid metabolism, it is present within this section as directly linked to the activation of plant defense responses. PLC together with the sequential action of diacylglycerol kinase (DGK) generate phosphatidic acid (PA), an early signal molecule involved in plant defense responses (Testerink and Munnik 2005). Another upregulated protein was MAP kinase 1 (GRMZM2G053987), essential in signal transduction and amplification in response to ISR (Bigeard and Hirt 2018).

In contrast, other components involved in signaling such as a putative calcium-binding protein CML13 (GRMZM2G324643), guanine-nucleotide-exchange protein (GRMZM2G058870), COP9 signalosome complex subunit 5b (CSN, GRMZM2G086801) and phytochrome A (GRMZM2G157727) were downregulated.

Priming proteins involved in hormone metabolism

From our selection of priming proteins (Fig. 6), we have found two different expressions corresponding to allene oxide synthase (AOS) isoforms. AOS1c (GRMZM2G033098) was upregulated whereas AOS2a (GRMZM2G002178) was downregulated. These proteins catalyze the first committed step of JA biosynthesis which converts 13-HPOT (13(S)-hydroperoxide octadecatrienoic acid) to a highly reactive allene oxide, which in the second committed step is converted to *cis*-12-oxo phytodienoic acid (OPDA) by allene oxide cyclase.

Regarding auxin metabolism, we have detected an upregulated aluminum-induced protein homolog 1 (GRMZM2G003762). However, we have not been able to elucidate its contribution to establishing the defense priming process.

On the other hand, a downregulated protein involved in ethylene metabolism was detected. This was a multiprotein-bridging factor 1a (MFB-1a) (GRMZM5G800112), which functions as a transcriptional co-activator in response to ethylene (Kim et al. 2007).

We have also detected in our assay a protein that seems to be involved in the interconversion of SA in methyl salicylate (MeSA). However, the protein responsible for this activity is encoded by a gene different (GRMZM2G168299) from that obtained in the transcriptomic assay (Agostini et al. 2019).

From these data, there is no clear involvement of a hormonal metabolic pathway activated by *T. atroviride* against *F. verticillioides*. This evidence would indicate that hormonal regulation and signaling may not require significant modifications at the protein level or are reflected on other regulatory mechanisms.

Priming proteins involved in transcriptional and translational regulation

It was also interesting for us to evaluate modifications of proteins involved in the regulation of transcriptional and translational processes due to the priming state. Transcription factors (TFs) are a group of proteins that regulate gene expression by binding to specific *cis*-acting elements in the promoters of target genes. Accordingly, we have found two TFs, such as a downregulated basic helix–loop–helix (bHLH) transcription factor 30 (GRMZM2G036092) and an upregulated homeodomain leucine zipper family IV protein (HD-Zip IV class, GRMZM2G116658).

In turn, we have also found proteins involved in RNA metabolism. One of these proteins was the downregulated Tudor-SN protein 1 (GRMZM2G136296) together with the upregulated Sm-like protein LSM2 (GRMZM2G092535). Tudor-SN is an evolutionarily conserved protein and plays diverse roles in the transcriptional and post-transcriptional regulation of gene expression. The Sm family proteins are essential part of RNP complexes and linked functionally to diverse cellular events of RNA metabolism, including nuclear RNA processing, pre-mRNA splicing, mRNA decay and miRNA biogenesis (Golisz et al. 2013).

As previously mentioned, and as part of the amino acid and protein metabolism category (Supplementary Fig. S2), several proteins related to protein synthesis, targeting, post-translational modifications and protein degradation also showed priming-related expression modulation. Among them, several ribosomal proteins (GRMZM2G145280, GRMZM2G127521, GRMZM2G179976, GRMZM2G068952, AC196489.3_FG002) change under priming condition. Some proteins connected to cellular targeting such as GRMZM2G081745 and GRMZM2G121022 also increase their expression under ISR. In addition, several proteins associated with post-translational modifications and protein degradation were also detected, such as GRMZM2G146819, GRMZM2G142334, GRMZM2G058560, GRMZM2G006416, GRMZM2G169182, GRMZM2G166646, GRMZM2G075488, GRMZM2G103266, GRMZM2G174572, GRMZM2G347743, GRMZM2G027378, GRMZM2G071010, GRMZM2G143782 and GRMZM2G028346. Overall, these

Journal : Large 425 | Article No : 3633 | Pages : 17 | MS Code : 3633 | Dispatch : 28-4-2021

are relevant changes involved in reprogramming cellular metabolism to deal with a threat (Fig. 6).

Priming proteins involved in response to stress

During the activation of the plant immune system, we observed a large number of upregulated proteins mainly related to biotic stress (Fig. 6). Among these, we have found a dirigent protein 11 (GRMZM2G420733) which has been involved in lignification, defense responses, and secondary metabolism (Ralph et al. 2007). In addition, we detected several upregulated pathogenesis-related proteins, such as PR10 (GRMZM2G112538, GRMZM2G112524 and GRMZM2G075283), PR-3 (GRMZM2G117989), endochitinase A (GRMZM2G051943), acidic endochitinase (GRMZM2G133781), stress-induced protein (GRMZM2G374971), osmotin-like protein OSM34 (GRMZM2G092474), β-1,3-glucanase (GRMZM2G125032) and chitinase chem 5 (GRMZM2G453805). The expression patterns for PR3, endochitinases (GRMZM2G051943 and GRMZM2G133781), stress-induced protein and β-1,3-glucanase correlate with those observed at the transcriptomic level (Agostini et al. 2019).

Redox metabolism

Redox metabolism plays an important role during the plant immune response. Therefore, most of the proteins detected (Fig. 6) were upregulated except for a protein disulfide isomerase-like 1–2 (GRMZM2G147210) which was downregulated in priming condition. As far as positively regulated proteins are concerned, we have found a probable nucleoredoxin 1 (GRMZM2G106344), a peroxiredoxin (GRMZM2G012276), a glutathione *S*-transferase (GST, GRMZM2G162486) and a NAD(P)H dehydrogenase (quinone) (FQR1, GRMZM2G082792). Evidently, as these results indicate, redox metabolism modulation seems to play an integral part in the initial activation of plant defense responses in silks from *Trichoderma*-elicited and *Fusarium*-infected plants.

Correlation of results from transcriptome and proteome analysis

To integrate our observations on a broader level for both the transcriptome and the proteome, we decided to correlate results obtained from the RNA-seq experiment (Agostini et al. 2019) with those obtained by HPLC–MS/MS analysis. In a Venn diagram (Fig. 8a), we compare the 652 differentially expressed genes (previously reported in Agostini et al. 2019) and the 609 genes coding for differentially expressed proteins detected in at least 1 condition (the present work). As a result, we detected that only 34 genes were regulated

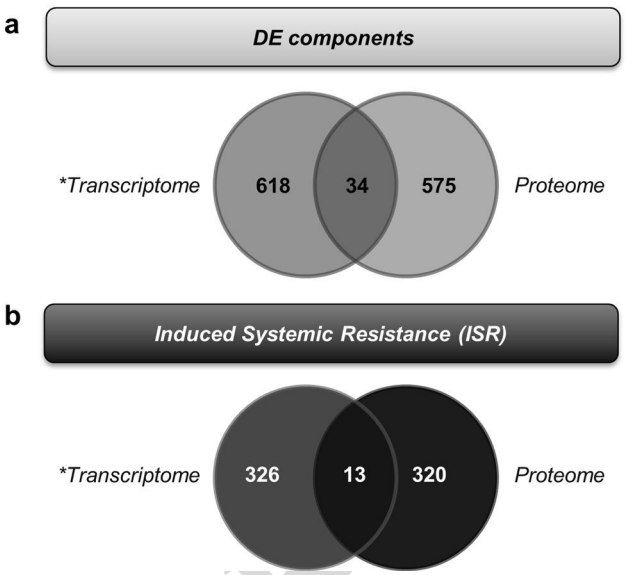

Fig. 8 **a** Venn Diagrams for the distribution of differentially expressed (DE) genes/proteins in the tripartite system *Z. mays—T. atroviride—F. verticillioides*. Transcriptome and proteome were analyzed by RNA-seq and HPLC–MS/MS experiments, respectively. **b** Distribution of selected priming components at the transcriptome and proteome levels in silks of maize plants under a state of induced systemic resistance (ISR). *Agostini et al. (2019)

at both the transcriptional and translational levels. When we analyzed the 34 differentially expressed genes detected in the 2 experiments, RNA-seq and proteomics; we found that 65.7% showed the same expression tendency. Among them, 61% showed increased levels of expression with respect to the control, both at the transcriptional and translational levels. All these were associated with biotic stress response mechanisms.

However, to compare and identify common elements in priming selection lists, accordingly to previously mentioned criteria, another Venn diagram (Fig. 8b) using priming genes identified by RNA-seq and genes coding for priming proteins detected by HPLC–MS/MS was constructed. Only 13 genes were detected at both the transcriptional and translational levels (Fig. 8b). Among the 13 priming genes detected in the 2 assays, there were a *probable inactive receptor kinase* (GRMZM2G394321), *mitochondrial dicarboxylate/tricarboxylate transporter DTC* (GRMZM2G042146), *α-humulene synthase* (ac205502.4_fg004), *acidic endochitinase* (GRMZM2G133781), *endochitinase A* (GRMZM2G051943), *osmotin-like protein OSM34* (GRMZM2G092474), *β-1,3-glucanase* (GRMZM2G125032), *PR-3* (GRMZM2G117989), *anthocyanidin 5,3-O-glucosyltransferase* (GRMZM2G063550), *glutathione S-transferase* (GRMZM2G162486), *chalcone synthase WHP1* (GRMZM2G151227), *stress-induced protein* (GRMZM2G374971) and *actin* (GRMZM2G053284).

Interestingly, 85% of the genes regulated at both the transcriptional and transcriptional levels presented the same expression tendency, that is, the activation or repression of the genes and proteins in question, being mainly proteins involved in biotic stress. Thus, despite the apparent non-relationship between the transcriptional and translational priming modifications, it is clear that the quicker response induced by *Trichoderma* against pathogen attack, is intricately regulated both in a transcriptional and translational fashion.

Discussion

Plant growth promotion and improvement of its immune response against a number of plant pathogens are the most significant benefits of *Trichoderma*–plant root colonization (Shoresh et al. 2010; Brotman et al. 2012). Therefore, several diseases caused by plant pathogens like vascular wilt induced by *Fusarium*, blight or gray mold triggered by *Botrytis*, anthracnose provoked by *Colletotrichum* spp., and several other plant fungal diseases, are counteracted by biocontrol treatment using *Trichoderma* strains worldwide (Sharma et al. 2017b).

The mechanisms reported for various *Trichoderma* species to activate ISR are diverse and depend on the actors involved in the interaction studied. However, in all cases, it is clear that after this interaction, a metabolic rearrangement in systemic tissues is necessary to respond to the circumstantial stress (Brotman et al. 2012; Mathys et al. 2012). To bring light to this issue, we have previously analyzed transcriptional changes in maize silks subjected to long-lasting priming states induced by *T. atroviride* 24 h after infection by the hemibiotrophic *F.verticillioides*.

To further assess our system, in this report, we describe morphological features as well as proteomic profiles of samples under the same previous conditions, contributing to a better understanding of the regulation levels controlling immunological responses in this system.

As expected, we detected very low correlation between both omics, despite they were taken from the same sample set. This is not rare, since it is known that gene expression is a dynamic process regulated at different extension both at the time and space levels. In addition, variations in the degree of translation are specific for each protein. Efficiency of the translation process can be affected by either the inherent nature of the mRNA molecule to be translated or an external environmental stimulus. Post-transcriptional events such as translation regulation and protein stability may be the main causes of weak correlations and variations in proteomic, transcriptomic, and genomic data (Sharma et al. 2017a).

In this context, it is worth mentioning that we have detected several proteins involved in RNA and protein synthesis that could be responsible for the above-mentioned discrepancy. Thus, expression modifications in Tudor-SN and Sm family proteins which are involved in nearly all pathways of gene expression, ranging from transcription to RNA silencing, might regulate stress-associated genes at their expression level (dit Frey et al. 2010; Golisz et al. 2013).

We have also detected several proteins involved in the translational process that appear upregulated in the priming state, which might suggest that the immediate response induced by *Trichoderma* to prevent pathogen dissemination, is protein translation activation, a process involved in the first line of defense (Fig. 6). On the other hand, regarding the post-translational level, one of our findings is the priming regulation of the multiprotein complex, Signalosome COP9 (CSN). This complex is involved in the regulation of protein degradation mediated by the proteosome and it may contribute to results obtained in our proteomic profile.

Due to their functions, these proteins could be key regulators of the priming components triggered by *Trichoderma* in silks. However, further studies are needed to explain their involvement in the low correlation between transcripts and protein profiles.

Overall, our results revealed the existence of a complex modulation in the expression of proteins, in response to the priming after the attack of *F. verticillioides*. This modulation results in the expression activation of proteins belonging to different functional categories like energy metabolism, cell wall structure and metabolism, amino acid and protein metabolism, and stress response (Fig. S2). This comprehensive reprogramming is likely intended to prevent pathogen spread by strengthening primary protective barriers and setting up a quick response to fungal intrusion.

Specifically comparing the expression tendency of functional categories between both omics under priming conditions (Fig. S2 of the present work and Fig. 5, of Agostini et al. 2019), we detected significant changes in expression profile for the *cell wall structure* and *lipid metabolism* categories. Therefore, it is basically in these groups where the differences between transcript and protein levels suggest the importance of post-transcriptional regulation as a means to offer a better performance against pathogen attack.

Thus, we specifically described some proteins from the phenylpropanoid and lignin biosynthetic pathways whose expression might be particularly regulated at the translational level since they were not selected as priming genes in our previous work. It is worth mentioning that the protein profiles observed in the priming state could explain the phenotypic results obtained regarding cell wall measurements along with phenolic compound and lignin content (Figs. 2, 3 and 4).

Journal : Large 425 | Article No : 3633 | Pages : 17 | MS Code : 3633 | Dispatch : 28-4-2021

Concerning flavonoid metabolism, FLS and chalcone isomerase are two of the enzymes overproduced in the priming condition and involved in the response to biotic stress (Fig. 7).

In addition, several enzymes related to lignin biosynthesis are also upregulated under these circumstances. Thus, 4CL, CCoAOMT, together with several peroxidases seem to be responsible for the higher lignin content in the presence of both pathogen and biocontrol agents (Fig. 3).

Accordingly, we also detected high levels of phenolic compounds in silk samples (Fig. 4) that might be involved in either lignin or phytoalexin biosynthesis. However, the increase in phenolic compound concentration was not exclusively induced by ISR, since it was also observed under infection with *F. verticillioides* and/or inoculation with *T. atroviride*. That is, both the biocontrol agent and the pathogen induce an increase in phenolic compounds at systemic level or in the local site of infection, respectively. This behavior is probably conditioned by the vast heterogeneity of compounds detected.

With the upregulation of several enzymes associated to the synthesis, processing and remodeling of the cell wall (β-expansin, mannose-1-phosphate guanylyl transferase 1), a clear cell wall cellulose deposition increment is observed in silks after ISR activation (Fig. 2). Along with lignin rearrangement, this would provide a strong cell wall to prevent pathogen entry and spread.

Surprisingly from our proteomic results, translation of some of the most studied genes of this pathway, PAL and chalcone synthase, were downregulated 24 h after infection with *F. verticillioides* in the priming state. Downregulation of chalcone synthase seems to be contradictory, since the increase in phenolic compound content with respect to the control condition remains constant in all different treatments, similar to results observed during flavonoid determination (data not shown). However, it has been reported that silencing chalcone synthase in maize leads to changes in lignin composition and content due to carbon flux redirection (Eloy et al. 2017). It would be probable that chalcone synthase downregulation along with the post-transcriptional

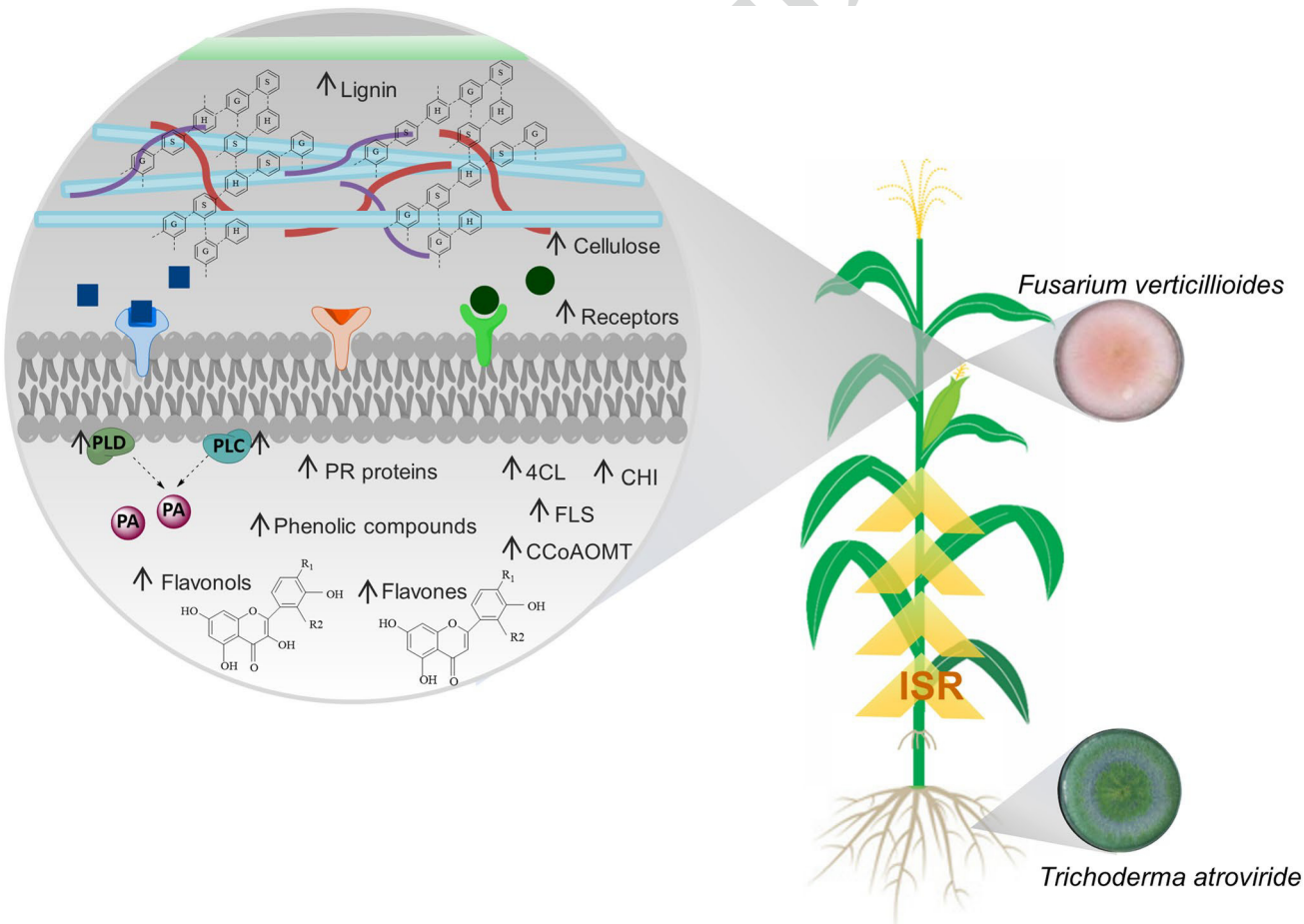

Fig. 9 Diagram representing the tripartite system *Z. mays, T. atroviride* and *F. verticillioides* analyzed and the mechanisms triggered by ISR activation

Journal : Large 425 | Article No : 3633 | Pages : 17 | MS Code : 3633 | Dispatch : 28-4-2021

stimulation of some other enzymes of the phenylpropanoid pathway is a result of ISR, somehow explaining observations connected to lignin content and cell wall width (Figs. 2 and 3).

On the other hand, it is well known that the multi-gene family of ZmPALs, the first committed enzyme in the phenylpropanoid biosynthesis pathway, is extensively regulated at several levels. In maize, this pathway also contributes to the biosynthesis of SA. Thus, maize differs from Arabidopsis or barley, in that the isochorismate pathway is the principal biosynthetic route for SA production; or soybean, in which the phenylpropanoid and isochorismate pathways are equally important (Ding and Ding 2020).

Therefore, it is likely that the observed downregulation in PAL expression together with the conversion in SA derivatives (due to the activation of the protein encoded by GRMZM2G168299) somehow explain the decrease in SA levels under ISR previously reported (Agostini et al. 2019). In the same way, previous evidence points to the involvement of JA/ET signaling activation as a response against *F. verticillioides* (Christensen et al. 2014; Lanubile et al. 2014) along with the activation of some proteins encoded by typical JA-responsive defense genes such as PR10 and chitinases, supporting the cross-talk and synergistic effects between the defense pathways mediated by SA and JA during the pathogenic infection under ISR.

This is the first analysis of proteomic and transcriptomic data obtained regarding the same priming conditions. From our analysis is clear that an integration between both datasets contributed to better understand the regulatory mechanisms controlling ISR and triggering quicker and more efficient defense responses, improving plant performance against hostile environments. A specific study of those proteins involved in post-transcriptional regulation will complement our understanding of such complex system.

A schematic summary of the most important changes observed is depicted in Fig. 9.

Author contribution statement RBA, VACB and SPR, conducted experimental work and analysis of the results. RBA, VACB, WAV, and SPR prepared the manuscript.

Supplementary Information The online version contains supplementary material available at https://doi.org/10.1007/s00425-021-03633-0.

Acknowledgements Agencia Nacional de Promoción Científica y Tecnológica ANPCyT PICT2014-0801, CONICET PIP 0028. WAV, VACB, and SPR are members of CIC from CONICET, Argentina. RBA is a doctoral fellow from CONICET.

References

Agostini RB, Postigo A, Rius SP, Rech GE, Campos-Bermudez VA, Vargas WA (2019) Long-lasting primed state in maize plants: Salicylic acid and steroid signaling pathways as key players in the early activation of immune responses in silks. Mol Plant-Microbe In 32(1):95–106

Bacon C, Glenn A, Yates I (2008) *Fusarium verticillioides*: managing the endophytic association with maize for reduced fumonisins accumulation. Toxin Rev 27(3–4):411–446

Bigeard J, Hirt H (2018) Nuclear signaling of plant MAPKs. Front Plant Sci 9:469

Borghi L, Kang J, de Brito FR (2019) Filling the gap: functional clustering of ABC proteins for the investigation of hormonal transport in planta. Front Plant Sci 10:422

Brotman Y, Lisec J, Méret M, Chet I, Willmitzer L, Viterbo A (2012) Transcript and metabolite analysis of the *Trichoderma*-induced systemic resistance response to *Pseudomonas syringae* in *Arabidopsis thaliana*. Microbiology 158(1):139–146

Christensen SA, Nemchenko A, Park Y-S, Borrego E, Huang P-C, Schmelz EA, Kunze S, Feussner I, Yalpani N, Meeley R (2014) The novel monocot-specific 9-lipoxygenase ZmLOX12 is required to mount an effective jasmonate-mediated defense against *Fusarium verticillioides* in maize. Mol Plant-Microbe In 27(11):1263–1276

Ding P, Ding Y (2020) Stories of salicylic acid: a plant defense hormone. Trends Plant Sci 25(6):549–565

dit Frey NF, Muller P, Jammes F, Kizis D, Leung J, Perrot-Rechenmann C, Bianchi MW (2010) The RNA binding protein Tudor-SN is essential for stress tolerance and stabilizes levels of stress-responsive mRNAs encoding secreted proteins in *Arabidopsis*. Plant Cell 22(5):1575–1591

Eloy NB, Voorend W, Lan W, Saleme MdLS, Cesarino I, Vanholme R, Smith RA, Goeminne G, Pallidis A, Morreel K, Nicomedes J Jr, Ralph J, Boerjan W (2017) Silencing *CHALCONE SYNTHASE* in maize impedes the incorporation of tricin into lignin and increases lignin content. Plant Physiol 173(2):998–1016

Ferrigo D, Raiola A, Rasera R, Causin R (2014) *Trichoderma harzianum* seed treatment controls *Fusarium verticillioides* colonization and fumonisin contamination in maize under field conditions. Crop Protect 65:51–56

Golisz A, Sikorski PJ, Kruszka K, Kufel J (2013) *Arabidopsis thaliana* LSM proteins function in mRNA splicing and degradation. Nucleic Acids Res 41(12):6232–6249

Kachroo A, Kachroo P (2009) Fatty acid–derived signals in plant defense. Annu Rev Phytopathol 47:153–176

Kim M-J, Lim G-H, Kim E-S, Ko C-B, Yang K-Y, Jeong J-A, Lee M-C, Kim CS (2007) Abiotic and biotic stress tolerance in Arabidopsis overexpressing the multiprotein bridging factor 1a (MBF1a) transcriptional coactivator gene. Biochem Biophys Res Commun 354(2):440–446

Lanubile A, Ferrarini A, Maschietto V, Delledonne M, Marocco A, Bellin D (2014) Functional genomic analysis of constitutive and inducible defense responses to *Fusarium verticillioides* infection in maize genotypes with contrasting ear rot resistance. BMC Genom 15(1):710

Li Y, Sun R, Yu J, Saravanakumar K, Chen J (2016) Antagonistic and biocontrol potential of *Trichoderma asperellum* ZJSX5003 against the maize stalk rot pathogen *Fusarium graminearum*. Indian J Microbiol 56(3):318–327

Ma L-S, Wang L, Trippel C, Mendoza-Mendoza A, Ullmann S, Moretti M, Carsten A, Kahnt J, Reissmann S, Zechmann B (2018) The *Ustilago maydis* repetitive effector Rsp3 blocks the antifungal activity of mannose-binding maize proteins. Nat Commun 9(1):1–15

Mandal SM, Chakraborty D, Dey S (2010) Phenolic acids act as signaling molecules in plant-microbe symbioses. Plant Signal Behav 5(4):359–368

Mathys J, De Cremer K, Timmermans P, Van Kerkhove S, Lievens B, Vanhaecke M, Cammue B, De Coninck B (2012) Genome-wide characterization of ISR induced in *Arabidopsis thaliana* by *Trichoderma hamatum* T382 against *Botrytis cinerea* infection. Front Plant Sci 3:108

Munkvold GP (2003) Cultural and genetic approaches to managing mycotoxins in maize. Annu Rev Phytopathol 41(1):99–116

Nawrocka J, Małolepsza U, Szymczak K, Szczech M (2018) Involvement of metabolic components, volatile compounds, PR proteins, and mechanical strengthening in multilayer protection of cucumber plants against *Rhizoctonia solani* activated by *Trichoderma atroviride* TRS25. Protoplasma 255(1):359–373

Nawrocka J, Gromek A, Małolepsza U (2019) Nitric oxide as a beneficial signaling molecule in *Trichoderma atroviride* TRS25-induced systemic defense responses of cucumber plants against *Rhizoctonia solani*. Front Plant Sci 10:421

Nogueira-Lopez G, Greenwood DR, Middleditch M, Winefield C, Eaton C, Steyaert JM, Mendoza-Mendoza A (2018) The apoplastic secretome of *Trichoderma virens* during interaction with maize roots shows an inhibition of plant defence and scavenging oxidative stress secreted proteins. Front Plant Sci 9:409

Park S-W, Kaimoyo E, Kumar D, Mosher S, Klessig DF (2007) Methyl salicylate is a critical mobile signal for plant systemic acquired resistance. Science 318(5847):113–116

Perez-Riverol Y, Csordas A, Bai J, Bernal-Llinares M, Hewapathirana S, Kundu DJ, Inuganti A, Griss J, Mayer G, Eisenacher M (2019) The PRIDE database and related tools and resources in 2019: improving support for quantification data. Nucleic Acids Res 47(D1):D442–D450

Pieterse CM, Zamioudis C, Berendsen RL, Weller DM, Van Wees SC, Bakker PA (2014) Induced systemic resistance by beneficial microbes. Annu Rev Phytopathol 52:347–375

Pottinger SE, Innes RW (2020) RPS5-mediated ddisease resistance: fundamental insights and translational applications. Annu Rev Phytopathol 58:139–160

Ralph SG, Jancsik S, Bohlmann J (2007) Dirigent proteins in conifer defense II: extended gene discovery, phylogeny, and constitutive and stress-induced gene expression in spruce (*Picea* spp.). Phytochemistry 68(14):1975–1991

Riboulet C, Guillaumie S, Méchin V, Bosio M, Pichon M, Goffner D, Lapierre C, Pollet B, Lefevre B, Martinant J (2009) Kinetics of phenylpropanoid gene expression in maize growing internodes: relationships with cell wall deposition. Crop Sci 49(1):211–223

Salas-Marina MA, Silva-Flores MA, Uresti-Rivera EE, Castro-Longoria E, Herrera-Estrella A, Casas-Flores S (2011) Colonization of *Arabidopsis* roots by *Trichoderma atroviride* promotes growth and enhances systemic disease resistance through jasmonic acid/ethylene and salicylic acid pathways. Eur J Plant Pathol 131(1):15–26

Saravanakumar K, Li Y, Yu C, Wang Q-q, Wang M, Sun J, Gao J-x, Chen J (2017) Effect of *Trichoderma harzianum* on maize rhizosphere microbiome and biocontrol of *Fusarium* stalk rot. Sci Rep 7(1):1–13

Segev N (2001) Ypt/rab GTPases: regulators of protein trafficking. Sci Signal 100:re11

Sharma V, Salwan R, Sharma P, Gulati A (2017a) Integrated translatome and proteome: approach for accurate portraying of widespread multifunctional aspects of *Trichoderma*. Front Microbiol 8:1602

Sharma V, Salwan R, Sharma PN, Kanwar S (2017b) Elucidation of biocontrol mechanisms of *Trichoderma harzianum* against different plant fungal pathogens: universal yet host specific response. Int J Biol Macromol 95:72–79

Shoresh M, Harman GE, Mastouri F (2010) Induced systemic resistance and plant responses to fungal biocontrol agents. Annu Rev Phytopathol 48:21–43

Testerink C, Munnik T (2005) Phosphatidic acid: a multifunctional stress signaling lipid in plants. Trends Plant Sci 10(8):368–375

Wang K-D, Borrego EJ, Kenerley CM, Kolomiets MV (2020) Oxylipins other than jasmonic acid are xylem-resident signals regulating systemic resistance induced by *Trichoderma virens* in maize. Plant Cell 32(1):166–185

Yedidia I, Benhamou N, Kapulnik Y, Chet I (2000) Induction and accumulation of PR proteins activityduring early stages of root colonizationby the mycoparasite *Trichoderma harzianum* strain T-203. Plant Physiol Biochem 38(11):863–873